bioRxiv preprint doi: https://doi.org/10.1101/2020.11.09.374934; this version posted November 9, 2020. The copyright holder for this preprint (which was not certified by peer review) is the author/funder, who has granted bioRxiv a license to display the preprint in perpetuity. It is made available under aCC-BY 4.0 International license.

Turing's diffusive threshold in random reaction-diffusion systems

Pierre A. Haas*
Mathematical Institute, University of Oxford, Woodstock Road, Oxford OX2 6GG, United Kingdom

Raymond E. Goldstein†
Department of Applied Mathematics and Theoretical Physics, Centre for Mathematical Sciences, University of Cambridge, Wilberforce Road, Cambridge CB3 0WA, United Kingdom

(Dated: November 9, 2020)

Abstract. Turing instabilities of reaction-diffusion systems can only arise if the diffusivities of the chemical species are sufficiently different. This threshold is unphysical in generic systems with $N = 2$ diffusing species, forcing experimental realizations of the instability to rely on fluctuations or additional non-diffusing species. Here we ask whether this diffusive threshold lowers for $N > 2$ to allow "true" Turing instabilities. Inspired by May's analysis of the stability of random ecological communities, we analyze the threshold for reaction-diffusion systems whose linearized dynamics near a homogeneous fixed point are given by a random matrix. In the numerically tractable cases of $N \leqslant 6$, we find that the diffusive threshold generically decreases as N increases and that these many-species instabilities generally require all species to be diffusing.

In 1952, Turing described the pattern-forming instability that now bears his name [1]: diffusion can destabilize a fixed point of a system of reactions that is stable in well-mixed conditions. Nigh on threescore and ten years on, the contribution of Turing's mechanism to chemical and biological morphogenesis remains debated, not least because of the *diffusive threshold* inherent in the mechanism: chemical species in reaction systems are expected to have roughly equal diffusivities, yet Turing instabilities cannot arise at equal diffusivities [2, 3]. It remains an open problem to determine how much of a diffusivity difference is required for generic systems to undergo this instability, yet this diffusive threshold has been recognized at least since reduced models of the Belousov–Zhabotinsky reaction [4, 5] only produced Turing patterns at unphysically large diffusivity differences.

For this reason, the first experimental realizations of Turing instabilities [6–8] obviated the threshold by using gel reactors that reduced the effective diffusivity of one species to create the required difference [9, 10]. (Analogously, membrane transport dynamics can increase the effective diffusivity difference in biological tissues [11].) Later work showed more explicitly how binding to an immobile substrate, or more generally, a third, non-diffusing species, can allow Turing instabilities even if the $N = 2$ diffusing species have equal diffusivities [12–14]. Such non-diffusing species continue to permeate more recent work on the network topology of Turing systems [15, 16].

Moreover, Turing instabilities need not be deterministic: fluctuation-driven instabilities in reaction-diffusion systems have noise-amplifying properties that allow their pattern amplitude to be comparable to that of deterministic Turing patterns [17], while the diffusive threshold for such stochastic instabilities may be lower than that for deterministic instabilities [18–20]. A synthetic bacterial population with $N = 2$ diffusing species that exhibits patterns in agreement with such a stochastic Turing instability, but does not satisfy the conditions for a deterministic instability [21], was reported recently.

These experimental instabilities relying on fluctuations or the dynamics of additional non-diffusing species are thus not instabilities in Turing's own image. Can such instabilities be realized instead in systems with $N > 2$ diffusing species? Equivalently, is the diffusive threshold lower in such systems? These questions have remained unanswered, perhaps because, in marked contrast to the textbook case $N = 2$ and the concomitant picture of an "inhibitor" out-diffusing an "activator" [22, 23], the complicated instability conditions for $N > 2$ [24] do not lend themselves to much analytical progress.

Here, we analyze the diffusive threshold for Turing instabilities with $2 \leqslant N \leqslant 6$ diffusing species. Inspired by May's work on the stability of random ecological communities [25], we analyze *random Turing instabilities* by sampling random matrices that represent the linearized reaction dynamics of otherwise unspecified reaction-diffusion systems. A semi-analytic approach for $N = 3$ shows that the diffusive threshold for instability is generically reduced compared to $N = 2$, and that two of the three diffusivities are equal at the threshold for instability. We extend these results to the remaining numerically tractable cases of reaction-diffusion systems with $4 \leqslant N \leqslant 6$ and two different diffusivities, showing that the diffusive threshold lowers further as N increases. Finally, we show that these many-species Turing instabilities generally require all species to diffuse.

We begin with the simplest case, $N = 2$, in which species u and v obey

$$\dot{u} = f(u, v) + d_u \nabla^2 u, \qquad \dot{v} = g(u, v) + d_v \nabla^2 v. \tag{1}$$

The conditions for Turing instability in this system [23] only depend on the four entries of the Jacobian

$$\mathsf{J} = \begin{pmatrix} f_u & f_v \\ g_u & g_v \end{pmatrix}, \tag{2}$$

the partial derivatives of the reaction system at a fixed point (u_*, v_*) of the homogeneous system. This fixed point is stable to homogeneous perturbations iff $J \equiv \det \mathsf{J} > 0$ and $I_1 \equiv \operatorname{tr} \mathsf{J} < 0$. A stable fixed point of this kind is unstable to a Turing instability only if $p \equiv -f_u g_v > 0$ [23]. Defining the diffusion coefficient ratio $D_2 = \max\{d_u/d_v, d_v/d_u\} \geqslant 1$, a Turing instability occurs iff these conditions hold along

bioRxiv preprint doi: https://doi.org/10.1101/2020.11.09.374934; this version posted November 9, 2020. The copyright holder for this preprint (which was not certified by peer review) is the author/funder, who has granted bioRxiv a license to display the preprint in perpetuity. It is made available under aCC-BY 4.0 International license.

with [26]

$$D_2 \geqslant D_2^* \equiv \left(\frac{\sqrt{J} + \sqrt{J+p}}{\min\{|f_u|, |g_v|\}} \right)^2 . \tag{3}$$

There is a diffusive threshold if D_2^* is large; to quantify this we introduce the *range* R of kinetic parameters,

$$R \equiv \frac{\max\{|f_u|, |f_v|, |g_u|, |g_v|\}}{\min\{|f_u|, |f_v|, |g_u|, |g_v|\}}. \tag{4}$$

Equivalently, $f_u, f_v, g_u, g_v \in I \equiv [-R, -1] \cup [1, R]$ up to scaling, with one parameter equal to ± 1 and one equal to $\pm R$. One deduces [26] that

$$D_2^* \leqslant D_2^{\max}(R) \equiv \left(R + \sqrt{R^2 - 1} \right)^2 , \tag{5}$$

as shown in Fig. 1(a). Note that $D_2^{\max} \to 1$ as $R \to 1$; in this limit, there is no diffusive threshold: $R \approx 1$ is a particular instance of the converse *fine-tuning problem* for the reaction kinetics that allows Turing instabilities at nearly equal diffusivities more generally [3]. If $R \gg 1$, then $D_2^{\max} = O(R^2)$. This does not imply the existence of a threshold, for this does not exclude most systems with range R having $D_2^* \ll D_2^{\max}$. The existence of the diffusive threshold therefore relates to the distribution of D_2^* for systems with range R.

To understand this distribution, we draw inspiration from May's analysis of the stability of large ecological communities [25]; large random Jacobians, corresponding to equilibria of otherwise unspecified population dynamics, are overwhelmingly likely to be unstable. By analogy, we study random Turing instabilities, sampling uniformly and independently the entries of random kinetic Jacobians corresponding to equilibria of otherwise unspecified reaction kinetics, and analyze the criteria for them to be Turing unstable. There is of course no more reason to expect the kinetic parameters to be independent or uniformly distributed than there is reason to expect the linearized population dynamics in May's analysis [25] to be independent or normally distributed. Yet, in the absence of experimental understanding of what the distributions of these parameters should be (in reaction-diffusion systems and in population dynamics), the potential of the random matrix approach to reveal stability principles has been amply demonstrated in population dynamics [29–37].

In Fig. 1(b), we estimate the probability distribution $P(D_2^*)$ for different values of R, sampling the kinetic parameters independently and uniformly from I and setting one of them equal to ± 1 and one equal to $\pm R$ [26]. Exact calculations [26] suggest that a natural quantifier of the threshold is the probability that D_2^* exceeds R,

$$\mathbb{P}(D_2^* \geqslant R) = \int_R^{D_2^{\max}} P(D_2^*)\, \mathrm{d}D_2^*. \tag{6}$$

Both from the estimates in Fig. 1(b) and by computing the integral in closed form [26], we find that $\mathbb{P}(D_2^* \geqslant R) > 0.97$ [Fig. 1(c)]. Thus, in the vast majority

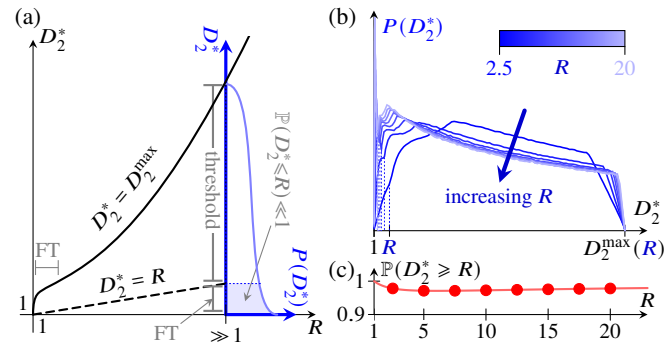

FIG. 1. Turing's diffusive threshold for $N = 2$. (a) Cartoon of the diffusive threshold and the fine-tuning (FT) problem for $R \approx 1$ and $R \gg 1$. (b) Distribution $P(D_2^*)$, supported on the (scaled) interval $[1, D_2^{\max}(R)]$, estimated for different R. (c) Plot of $\mathbb{P}(D_2^* \geqslant R)$ against R, revealing the diffusive threshold. Markers: estimates from the distributions in Fig. 1(b); solid line: exact result [26].

of cases, the diffusivity ratio is "large"; conversely, Turing instabilities at small diffusive threshold require fine-tuning [Fig. 1(a)]. This expresses Turing's threshold for two-species systems.

To investigate how this diffusive threshold changes with N we consider next the $N = 3$ system

$$\dot{u} = f(u, v, w) + d_u \nabla^2 u, \tag{7a}$$

$$\dot{v} = g(u, v, w) + d_v \nabla^2 v, \tag{7b}$$

$$\dot{w} = h(u, v, w) + \nabla^2 w, \tag{7c}$$

where we have rescaled space to set $d_w = 1$. We introduce the matrix of diffusivities and the reaction Jacobian,

$$\mathsf{D} = \begin{pmatrix} d_u & 0 & 0 \\ 0 & d_v & 0 \\ 0 & 0 & 1 \end{pmatrix}, \qquad \mathsf{J} = \begin{pmatrix} f_u & f_v & f_w \\ g_u & g_v & g_w \\ h_u & h_v & h_w \end{pmatrix}, \tag{8}$$

in which the entries of J are again the partial derivatives evaluated at a fixed point (u_*, v_*, w_*) of the homogeneous system. This system is unstable to a Turing instability if J is stable, but, for some eigenvalue $-k^2 < 0$ of the Laplacian, $\bar{\mathsf{J}}(k^2) = \mathsf{J} - k^2 \mathsf{D}$ is unstable [3]. More precisely, a Turing instability arises when a real eigenvalue of $\mathsf{J}(k^2)$ crosses zero, i.e. when $\mathcal{J}(k^2) \equiv \det \bar{\mathsf{J}}(k^2) = 0$, and therefore arises first at a wavenumber $k = k_*$ with $\mathcal{J}(k_*^2) = \partial \mathcal{J} / \partial k^2 (k_*^2) = 0$ [3]. Hence $\mathcal{J}$, a cubic polynomial in k^2, must have a double root at $k^2 = k_*^2 > 0$, so its discriminant [28] must vanish. This discriminant is a sextic polynomial in d_u, d_v,

$$\Delta(d_u, d_v) = \sum_{m=0}^{4} \sum_{n=0}^{4} \delta_{mn} d_u^m d_v^n, \tag{9}$$

where $\delta_{00} = \delta_{10} = \delta_{01} = \delta_{34} = \delta_{43} = \delta_{44} = 0$ and (complicated) expressions for the 19 non-zero coefficients can be found in terms of the entries of J using MATHEMATICA (Wolfram, Inc.). The double root of $\mathcal{J}$ corresponding to (d_u, d_v) on the curve $\Delta(d_u, d_v) = 0$ is $K(d_u, d_v)$.

bioRxiv preprint doi: https://doi.org/10.1101/2020.11.09.374934; this version posted November 9, 2020. The copyright holder for this preprint (which was not certified by peer review) is the author/funder, who has granted bioRxiv a license to display the preprint in perpetuity. It is made available under aCC-BY 4.0 International license.

Determining the diffusive threshold for Turing instability in Eqs. (7) thus requires solving the problem

$$\text{minimize } D_3(d_u, d_v) \quad \text{subject to} \begin{cases} \Delta(d_u, d_v) = 0, \\ K(d_u, d_v) > 0, \end{cases} \tag{10}$$

in which the diffusion coefficient ratio is

$$D_3(d_u, d_v) = \max\{d_u, 1/d_u, d_v, 1/d_v, d_u/d_v, d_v/d_u\}. \tag{11}$$

Direct numerical solution of this constrained optimisation problem is obviously not a feasible approach, since we ultimately want to obtain statistics for the minimal value D_3^* and the corresponding (d_u^*, d_v^*). We therefore solve this problem semi-analytically in what follows.

Before doing so, we must note the following: the necessary and sufficient (Routh–Hurwitz) conditions for J to be stable include $I_1 \equiv \operatorname{tr}\mathsf{J} < 0$ and $J \equiv \det\mathsf{J} < 0$ [23]. By definition, $\bar{\mathsf{J}}(k_*^2)$ has one zero eigenvalue. The other two eigenvalues are either real or two complex conjugates λ, λ^*. In the second case, they are both stable since $2\operatorname{Re}(\lambda) = 0 + \lambda + \lambda^* = \operatorname{tr}\bar{\mathsf{J}}(k_*^2) = I_1 - k_*^2 \operatorname{tr}\mathsf{D} < I_1 < 0$. Hence Eqs. (7) are not unstable to an oscillatory (Turing–Hopf) instability at (d_u^*, d_v^*), so, by minimality of (d_u^*, d_v^*), the system destabilizes to a Turing instability there. Moreover, since $\mathcal{J}$ has leading coefficient $-d_u d_v$ and $\mathcal{J}(0) = J < 0$, the double root $K(d_u, d_v)$ varies continuously with d_u, d_v and cannot change sign on a branch of $\Delta(d_u, d_v) = 0$ in the positive (d_u, d_v) quadrant.

This last remark implies that, at a local minimum of $D_3(d_u, d_v)$ on $\Delta(d_u, d_v) = 0$, one of the following occurs: (i) $\Delta(d_u, d_v) = 0$ is tangent to a contour of $D_3(d_u, d_v)$; (ii) $\Delta(d_u, d_v)$ intersects a vertex of a contour of $D_3(d_u, d_v)$; (iii) $\Delta(d_u, d_v)$ is singular. The contours of $D_3(d_u, d_v)$ are drawn in Fig. 2(a) and show that tangency to a contour in case (i) requires $\mathrm{d}d_u = 0$ or $\mathrm{d}d_v = 0$ or $\mathrm{d}d_v/\mathrm{d}d_u = d_v/d_u$. Since $\Delta(d_u, d_v) = 0$, the chain rule reads $0 = \mathrm{d}\Delta = (\partial\Delta/\partial d_u)\,\mathrm{d}d_u + (\partial\Delta/\partial d_v)\,\mathrm{d}d_v$. Hence there are two subcases: (a) $\partial\Delta/\partial d_v = 0$ or $\partial\Delta/\partial d_u = 0$ and (b) $d_u\partial\Delta/\partial d_u + d_v\partial\Delta/\partial d_v = 0$. In subcase (a), Δ viewed as a polynomial in d_v or d_u has a double root, and so its discriminant [28] must vanish. On removing zero roots, this discriminant of a discriminant is found to be a polynomial of degree 20 in d_u or d_v, respectively; complicated expressions for its coefficients in terms of the non-zero coefficients δ_{mn} in Eq. (9) are obtained using Mathematica. Similarly, in subcase (b), the resultant [28] of Δ and $d_u\partial\Delta/\partial d_u + d_v\partial\Delta/\partial d_v$, viewed as polynomials in d_u or d_v must vanish. This resultant is another polynomial of degree 20 in d_v or d_u. Next, in case (ii), $d_u = 1$ or $d_v = 1$ or $d_u = d_v$ [Fig. 2(a)], which reduces Δ to three different polynomials of degree 6 in the single variable d_v, d_u, or $d = d_u = d_v$, respectively. Finally, in case (iii), at a singular point, $\Delta = \partial\Delta/\partial d_u = \partial\Delta/\partial d_v = 0$, and we are back in case (i), subcase (a). Thus, we have reduced finding candidates for local minima in (10) to solving polynomial equations; the global minimum is found among those local minima with $K(d_u, d_v) > 0$ [38].

We implement this semi-analytical approach as described in the Supplemental Material [26], and sample random systems

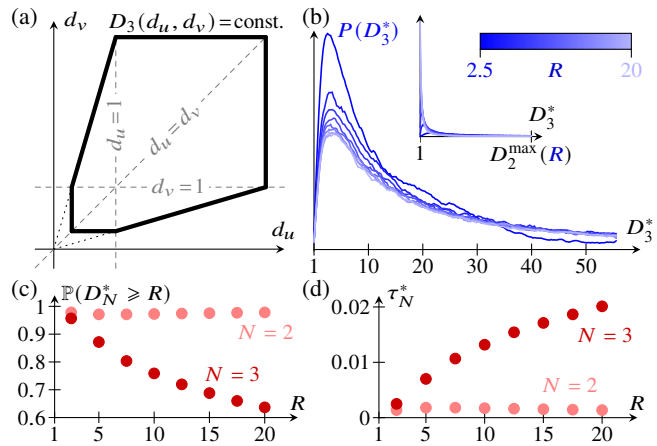

FIG. 2. Results for $N = 3$. (a) Contours of $D_3(d_u, d_v)$ in the positive (d_u, d_v) quadrant. (b) Smoothed distribution $P(D_3^*)$, estimated for different R. Inset: same plot scaled to $[1, D_2^{\max}(R)]$ for comparison to $N = 2$ in Fig. 1(a). (c) Plot of $\mathbb{P}(D_N^* \geqslant R)$ against R for $N \in \{2, 3\}$, revealing lowering of the diffusive threshold for $N = 3$ compared to $N = 2$. (d) Probability τ_N^* of a random kinetic Jacobian having a Turing instability with $D_N^* \leqslant R$ plotted against R, for $N \in \{2, 3\}$.

similarly to the two-species case, drawing the entries of J in Eq. (8) uniformly and independently at fixed range R.

Strikingly, D_3^* is attained at a contour vertex, corresponding to case (ii) above: numerically [26], we only found global minima of this type. In particular, the minimising systems come in two flavors: those with two "fast" diffusers and one "slow" diffuser, and those with one "fast" diffuser and two "slow" diffusers. Systems with a non-diffusing species are a limit of the former; this point will be discussed below. The latter arise for example in models of scale pattern formation in fish and lizards [39, 40], in which short-range pigments respectively activate and inhibit a long-range factor.

The distribution of D_3^*, shown for different values of R in Fig. 2(b), is rather different from that of D_2^* [Figs. 1(a) and 2(b), inset]. Even though the support of the distribution of D_3^* does not appear to be bounded, the probability $\mathbb{P}(D_3^* \geqslant R)$ is reduced compared to the two-species case [Fig. 2(c)]. Hence the diffusive threshold lowers for $N = 3$ compared to $N = 2$. A random Jacobian with $N = 3$ is less likely to be Turing unstable than one with $N = 2$ (essentially because there are more conditions on the parameters for $N = 3$). However, because the threshold for Turing instability is so high for $N = 2$, and lowered for $N = 3$, a random kinetic Jacobian is vastly more likely to have a Turing instability with $D_N^* \leqslant R$ for $N = 3$ than for $N = 2$, even though the latter is more likely to have a Turing instability of any kind.

To extend these results to $N > 3$ diffusing species, we consider the (linearized) reaction-diffusion system

$$\dot{\boldsymbol{u}} = \mathsf{J} \cdot \boldsymbol{u} + \mathsf{D} \cdot \nabla^2 \boldsymbol{u}, \tag{12}$$

where J is a random kinetic Jacobian, and D is a diagonal matrix of diffusivities. Even with the semi-analytical approach developed above, such systems cannot be analyzed for general D: not even for $N = 4$ were we able to obtain closed

bioRxiv preprint doi: https://doi.org/10.1101/2020.11.09.374934; this version posted November 9, 2020. The copyright holder for this preprint (which was not certified by peer review) is the author/funder, who has granted bioRxiv a license to display the preprint in perpetuity. It is made available under aCC-BY 4.0 International license.

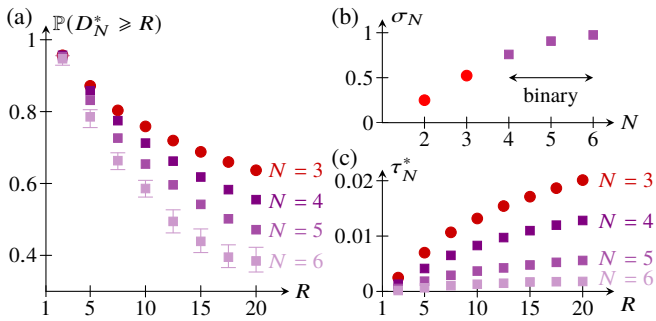

FIG. 3. Results for "binary" systems with $4 \leqslant N \leqslant 6$. (a) $\mathbb{P}(D_N^* \geqslant R)$ against R for $3 \leqslant N \leqslant 6$, revealing further lowering of the diffusive threshold compared to the case $N = 3$. (b) Probability σ_N of a random stable kinetic Jacobian having a (binary, if $N > 3$) Turing instability plotted against N and averaged over R. (c) Probability τ_N^* of a random kinetic Jacobian having a Turing instability with $D_N^* \leqslant R$ plotted against R, for $3 \leqslant N \leqslant 6$ [41].

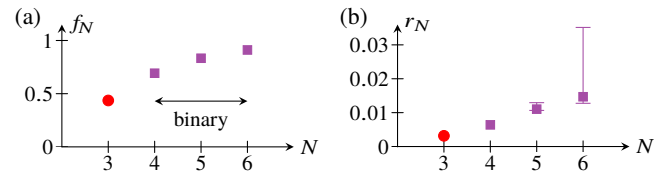

FIG. 4. "Slow" diffusers in binary Turing instabilities with $3 \leqslant N \leqslant 6$. (a) Proportion f_N of Turing unstable systems with $n \geqslant 2$ "fast" diffusers plotted against N, averaged over R. (b) Proportion r_N of systems for which j has a positive eigenvalue, plotted against N, averaged over R [41].

forms of the required polynomial coefficients. To make further progress, we therefore restrict to "binary" D in which the N diffusivities take two different values only. Above, we showed that D_3^* is attained for such binary D. The discriminant $\Delta(\mathsf{D})$ of $\mathsf{J} - k^2\mathsf{D}$ thus reduces to $2^{N-1} - 1$ different polynomials in one variable, the coefficients of which we obtained in closed form for $4 \leqslant N \leqslant 6$. Solving $\Delta(\mathsf{D}) = 0$ determines the threshold for Turing instability in these binary systems as in the case $N = 3$ discussed above [42].

The diffusive threshold lowers further in these binary systems with $4 \leqslant N \leqslant 6$, as shown in Fig. 3(a). The fact that most stable random kinetic Jacobians undergo such a binary Turing instability [Fig. 3(b)] suggests that these provide a useful picture of the diffusive threshold. Since the probability of random kinetic Jacobians being Turing unstable decreases as N increases, the probability of them being Turing unstable with D_N^* also decreases, despite the lowering of the threshold [Fig. 3(c)].

Again, the different species in these binary systems separate into "fast" and "slow" diffusers. The diffusion of the slow diffusers cannot however in general be ignored. Up to reordering the species and rescaling space,

$$\mathsf{D} = \left(\begin{array}{c|c} \mathsf{I} & 0 \\ \hline 0 & d\mathsf{I} \end{array}\right), \qquad \mathsf{J} = \left(\begin{array}{c|c} \mathsf{J}_{11} & \mathsf{J}_{12} \\ \hline \mathsf{J}_{21} & \mathsf{J}_{22} \end{array}\right), \tag{13}$$

where $d < 1$ is the common diffusivity of the slow diffusers. If $d = 0$, recent results [43] on general Turing instabilities with non-diffusing species imply that $\det\left(\mathsf{J} - k^2\mathsf{D}\right) = \det \mathsf{J}_{22} \det\left(\mathsf{j} - k^2\mathsf{I}\right)$, with $\mathsf{j} = \mathsf{J}_{11} - \mathsf{J}_{12}\mathsf{J}_{22}^{-1}\mathsf{J}_{21}$. Additionally, Turing instability at $d = 0$ requires J_{22} to be stable: if it is not, instabilities arise at arbitrarily small and therefore unphysical lengthscales [43]. In that case, $\det \mathsf{J}_{22} \neq 0$, and there is a Turing instability with $d = 0$ only if j has a positive eigenvalue. Although the proportion of Turing unstable systems with $n \geqslant 2$ fast diffusers that could in principle still undergo a Turing instability with $d = 0$ increases with N [Fig. 4(a)], the proportion of systems for which j has a positive eigenvalue is small [Fig. 4(b)]. Hence the Turing instabilities with $N > 3$ species considered here generally require all species to diffuse, and are more general than the instabilities of systems with non-diffusing species realized in gel reactors [6–8] and analyzed recently [43].

In this Letter, we have analyzed random Turing instabilities to show how the diffusive threshold that has hampered experimental efforts to generate "true" Turing instabilities in systems of $N = 2$ diffusing species is lowered for $N \geqslant 3$. All of this does not, however, explain the existence of a "large" threshold in the first place—even though Turing instabilities at equal diffusivities are impossible [2, 3], there is no *a priori* reason why the threshold should be "large". This can be understood asymptotically: Let $\mathsf{J} = O(1)$ be a Turing unstable kinetic Jacobian, with an eigenvalue λ destabilising at nearly equal diffusivities $\mathsf{D} = \mathsf{I} + \mathsf{d}$ with $\mathsf{d} = o(1)$. Because $\mathsf{J} - k^2\mathsf{I}$ has a stable eigenvalue $\lambda - k^2$ and $-k^2\mathsf{d} \ll \mathsf{J} - k^2\mathsf{I}$, the corresponding eigenvalue of $\mathsf{J} - k^2\mathsf{D} = \left(\mathsf{J} - k^2\mathsf{I}\right) - k^2\mathsf{d}$ can only be positive if $\lambda - k^2 = o(1)$ i.e. if $\lambda = o(1)$ and $k^2 = o(1)$ since $\mathrm{Re}(\lambda) < 0$. Hence J and $\mathsf{J} - k^2\mathsf{I}$ have a zero eigenvalue at leading order. Additionally, the eigenvalue correction from $-k^2\mathsf{d} = o\left(k^2\right)$ must be $O\left(k^2\right)$ at least. This occurs iff the (leading-order) zero eigenspace of $\mathsf{J} - k^2\mathsf{I}$ and J is defective [44, 45]. This extends an argument of Ref. [3]. The generic case is therefore $\mathsf{J} = \mathsf{J}_0 + O(\varepsilon)$, where $\varepsilon \ll 1$ and J_0 has a defective double zero eigenvalue, so that J has two $O(\sqrt{\varepsilon})$ eigenvalues [44], assumed to be stable. With $k = O(\varepsilon^\kappa)$, $\mathsf{d} = O\left(\varepsilon^\delta\right)$, destabilizing one of these requires, by the above, $-k^2\mathsf{d} \gtrsim O(\varepsilon)$ and $-k^2\mathsf{I} \lesssim O(\sqrt{\varepsilon})$, i.e. $2\kappa + \delta \leqslant 1$ and $\kappa \geqslant 1/4$. Hence $\delta \leqslant 1/2$; in particular, $\mathsf{D} - \mathsf{I} \gtrsim O(\sqrt{\varepsilon}) \gg O(\varepsilon) = \mathsf{J} - \mathsf{J}_0$, and so the diffusive threshold is "large" in this asymptotic limit. Understanding the mechanism by which the threshold arises more generally and lowers as N increases remains an open problem, as do extending previous work [16, 46] on the robustness of Turing patterns to $N \geqslant 3$ and identifying chemical or biological pattern forming systems with $N \geqslant 3$ in which the "true" Turing instabilities discussed here can be realized experimentally.

We thank N. Goldenfeld, A. Krause, and P. K. Maini for discussions. This work was supported in part by a Nevile Research Fellowship from Magdalene College, Cambridge, and a Hooke Research Fellowship (P.A.H.), Established Career Fellowship EP/M017982/1 from the Engineering and Physical Sciences Research Council and Grant 7523 from the Marine Microbiology Initiative of the Gordon and Betty Moore Foundation (R.E.G.).

bioRxiv preprint doi: https://doi.org/10.1101/2020.11.09.374934; this version posted November 9, 2020. The copyright holder for this preprint (which was not certified by peer review) is the author/funder, who has granted bioRxiv a license to display the preprint in perpetuity. It is made available under aCC-BY 4.0 International license.

* haas@maths.ox.ac.uk
† r.e.goldstein@damtp.cam.ac.uk

[1] A. M. Turing, The chemical basis of morphogenesis, Phil. Trans. R. Soc. B **237**, 37 (1952).
[2] J. A. Vastano, J. E. Pearson, W. Horsthemke, and H. L. Swinney, Chemical pattern formation with equal diffusion coefficients, Phys. Lett. A **124**, 320 (1987).
[3] J. E. Pearson and W. Horsthemke, Turing instabilities with nearly equal diffusion coefficients, J. Chem. Phys. **90**, 1588 (1989).
[4] P. K. Becker and R. J. Field, Stationary concentration patterns in the oregonator model of the Belousov–Zhabotinskii reaction, J. Phys. Chem. **89**, 118 (1985).
[5] A. B. Rovinskii, Turing bifurcation and stationary patterns in the ferroin-catalyzed Belousov–Zhabotinskii reaction, J. Phys. Chem. **91**, 4606 (1987).
[6] V. Castets, E. Dulos, J. Boissonade, and P. De Kepper, Experimental evidence of a sustained standing Turing-type nonequilibrium chemical pattern, Phys. Rev. Lett. **64**, 2953 (1990).
[7] P. De Kepper, V. Castets, E. Dulos, and J. Boissonade, Turing-type chemical patterns in the chlorite-iodide-malonic acid reaction, Physica D **49**, 161 (1991).
[8] Q. Ouyang and H. L. Swinney, Transition from a uniform state to hexagonal and striped Turing patterns, Nature **352**, 610 (1991).
[9] I. Lengyel and I. R. Epstein, Modeling of Turing structures in the chloride-iodid-malonic acid-starch reaction system, Science **251**, 650 (1991).
[10] E. Dulos, J. Boissonade, J. J. Perraud, B. Rudovics, and P. De Kepper, Chemical morphogenesis: Turing patterns in an experimental chemical system, Acta Biother. **44**, 249 (1996).
[11] P. Recho, A. Hallou, and E. Hannezo, Theory of mechanochemical patterning in biphasic biological tissues, Proc. Natl. Acad. Sci. USA **116**, 5344 (2019).
[12] I. Lengyel and I. R. Epstein, A chemical approach to designing Turing patterns in reaction-diffusion systems, Proc. Natl. Acad. Sci. USA **89**, 3977 (1992).
[13] J. E. Pearson, Pattern formation in a $(2+1)$-species activator-inhibitor-immobilizer system, Physica A **188**, 178 (1992).
[14] K. Korvasová, E. A. Gaffney, P. K. Maini, M. A. Ferreira, and V. Klika, Investigating the Turing conditions for diffusion-driven instability in the presence of a binding immobile substrate, J. Theor. Biol. **367**, 286 (2015).
[15] L. Marcon, X. Diego, J. Sharpe, and P. Müller, High-throughput mathematical analysis identifies Turing networks for patterning with equally diffusing signals, eLife **5**, e14022 (2016).
[16] X. Diego, L. Marcon, P. Müller, and J. Sharpe, Key features of Turing systems are determined purely by network topology, Phys. Rev. X **8**, 021071 (2018).
[17] T. Biancalani, F. Jafarpour, and N. Goldenfeld, Giant amplification of noise in fluctuation-induced pattern formation, Phys. Rev. Lett. **118**, 018101 (2017).
[18] T. Butler and N. Goldenfeld, Robust ecological pattern formation induced by demographic noise, Phys. Rev. E **80**, 030902(R) (2009).
[19] T. Biancalani, D. Fanelli, and F. Di Patti, Stochastic Turing patterns in the Brusselator model, Phys. Rev. E **81**, 046215 (2010).
[20] T. Butler and N. Goldenfeld, Fluctuation-driven Turing patterns, Phys. Rev. E **84**, 011112 (2011).
[21] D. Karig, K. M. Martini, T. Lu, N. A. DeLateur, N. Goldenfeld, and R. Weiss, Stochastic Turing patterns in a synthetic bacterial population, Proc. Natl. Acad. Sci. USA **115**, 6572 (2018).
[22] A. J. Koch and H. Meinhardt, Biological pattern formation: from basic mechanisms to complex structures, Rev. Mod. Phys. **66**, 1481 (1994).
[23] J. D. Murray, in *Mathematical Biology* (Springer, Berlin, Germany, 2002) Vol. I, Appendix B.1, pp. 507–509 and Vol. II, Chap. 2, pp. 71–140, 3rd ed.
[24] R. A. Satnoianu, M. Menzinger, and P. K. Maini, Turing instabilities in general systems, J. Math. Biol. **41**, 493 (2000).
[25] R. M. May, Will a large complex ecosystem be stable?, Nature **238**, 413 (1972).
[26] See Supplemental Material at [url to be inserted], which includes Refs. [23, 27, 28], for details of calculations for $N = 2$ and of the numerical implementation and for `python3` code.
[27] F. Johansson, *`mpmath`: a `python` library for arbitrary-precision floating-point arithmetic* (version 1.1.0, 2018).
[28] C.-K. Yap, in *Fundamental Problems in Algorithmic Algebra* (Oxford University Press, Oxford, England, 2000) Chap. 6 & 7, pp. 141–218.
[29] S. Allesina and S. Tang, Stability criteria for complex ecosystems, Nature **482**, 205 (2012).
[30] J. Grilli, T. Rogers, and S. Allesina, Modularity and stability in ecological communities, Nat. Commun. **7**, 12031 (2016).
[31] T. Gibbs, J. Grilli, T. Rogers, and S. Allesina, Effect of population abundances on the stability of large random ecosystems, Phys. Rev. E **98**, 022410 (2018).
[32] C. A. Serván, J. A. Capitán, J. Grilli, K. E. Morrison, and S. Allesina, Coexistence of many species in random ecosystems, Nat. Ecol. Evol. **2**, 1237 (2018).
[33] S. Butler and J. P. O'Dwyer, Stability criteria for complex microbial communities, Nat. Commun. **9**, 2970 (2018).
[34] L. Stone, The feasibility and stability of large complex biological networks: a random matrix approach, Sci. Rep. **8**, 8246 (2018).
[35] D. S. Maynard, C. A. Serván, J. A. Capitán, and S. Allesina, Phenotypic variability promotes diversity and stability in competitive communities, Ecol. Lett. **22**, 1776 (2019).
[36] P. A. Haas, N. M. Oliveira, and R. E. Goldstein, Subpopulations and stability in microbial communities, Phys. Rev. Research **2**, 022036(R) (2020).
[37] J. W. Barron and T. Galla, Dispersal-induced instability in complex ecosystems, arXiv:2003.04206 (2020).
[38] In case (i), the roots only correspond to local minima if additionally $d_u, d_v > 1$ or $d_u, d_v < 1$ in subcase (a) and $d_u < 1 < d_v$ or $d_v < 1 < d_u$ in subcase (b) [Fig. 2(a)].
[39] A. Nakamasu, G. Takahashi, A. Kanbe, and S. Kondo, Interactions between zebrafish pigment cells responsible for the generation of Turing patterns, Proc. Natl. Acad. Sci. USA **106**, 8429 (2009).
[40] L. Manukyan, S. A. Montandon, A. Fofonjka, S. Smirnov, and M. C. Milinkovitch, A living mesoscopic cellular automaton made of skin scales, Nature **544**, 173 (2017).
[41] The asymmetric error bars in Figs. 3 and 4 show 95% confidence intervals, corrected for systems for which the numerics failed and larger than the plot markers.
[42] For $N > 3$, coexistence of Turing and Turing–Hopf instabilities is possible; we discard those very few systems that undergo a Turing–Hopf instability first, but include them in error estimates.
[43] S. Smith and N. Dalchau, Model reduction enables Turing instability analysis of large reaction–diffusion models, J. R. Soc. Interface **15**, 20170805 (2018).
[44] E. J. Hinch, in *Perturbation Methods* (Cambridge University Press, Cambridge, UK, 1991) Chap. 1.6, pp. 15–18.
[45] V. B. Lidskii, Perturbation theory of non-conjugate operators, USSR Comp. Math. Math. Phys. **6**, 73 (1966).
[46] N. S. Scholes, D. Schnoerr, M. Isalan, and M. P. H. Stumpf, A comprehensive network atlas reveals that Turing patterns are common but not robust, Cell Systems **9**, 243 (2019).

bioRxiv preprint doi: https://doi.org/10.1101/2020.11.09.374934; this version posted November 9, 2020. The copyright holder for this preprint (which was not certified by peer review) is the author/funder, who has granted bioRxiv a license to display the preprint in perpetuity. It is made available under aCC-BY 4.0 International license.

Turing's diffusive bottleneck in random reaction-diffusion systems
— Supplemental Material —

Pierre A. Haas
Mathematical Institute, University of Oxford, Woodstock Road, Oxford OX2 6GG, United Kingdom

Raymond E. Goldstein
Department of Applied Mathematics and Theoretical Physics, Centre for Mathematical Sciences, University of Cambridge, Wilberforce Road, Cambridge CB3 0WA, United Kingdom

This Supplemental Material is divided into two sections. The first section provides details of calculations for $N = 2$. The second section gives details of the numerical implementation.

I. DETAILS OF CALCULATIONS FOR $N = 2$

A. Derivation of Eq. (3)

The form of the condition for Turing instability in Eq. (3) follows from that in Eq. (2.26) on page 85 of Vol. II of Ref. [S1] which, in our notation, reads

$$f_u + dg_v \geqslant 2\sqrt{dJ}, \tag{S1}$$

a quadratic in $d = d_u/d_v$. Hence

$$\sqrt{d} \gtrless \frac{\sqrt{J} \pm \sqrt{J - f_u g_v}}{g_v} \quad \text{if } g_v \gtrless 0. \tag{S2}$$

Now, if $g_v \gtrless 0$, then $|f_u| \gtrless |g_v|$ because $I_1 < 0$ and $p > 0$. Equation (3) then follows, since

$$\frac{g_v}{\sqrt{J} - \sqrt{J+p}} = \frac{\sqrt{J} + \sqrt{J+p}}{f_u}. \tag{S3}$$

B. Derivation of Eq. (5)

Equation (3) shows that D_2^* is continuous on I^4, so attains its maximum value on that domain. Since $p > 0$ and $J > 0$, $q \equiv -f_v g_u > 0$, so that $J + p = q$. Now D_2^* only depends on f_v, g_u through q, and, by direct computation from Eq. (3),

$$\frac{\partial D_2^*}{\partial q} = \frac{D_2^*}{\sqrt{J(J+p)}} > 0. \tag{S4}$$

Hence D_2^* increases with q, so $(f_v, g_u) = \pm(R, -R)$ at the maximum.

Now assume that $|f_u| \geqslant |g_v|$. Since $I_1 < 0$ and $|f_u| \geqslant |g_v|$, it follows that $f_u < 0$ and $g_v > 0$. Then

$$\frac{\partial D_2^*}{\partial f_u} = \frac{\sqrt{J} + \sqrt{q}}{g_v\sqrt{J}} > 0, \quad \frac{\partial D_2^*}{\partial g_v} = -\frac{\left(\sqrt{J} + \sqrt{q}\right)^3}{g_v^3\sqrt{J}} < 0, \tag{S5}$$

and so $(f_u, g_v) = (1, -1)$ at the maximum. If $|f_u| \leqslant |g_v|$, we similarly find that $(f_u, g_v) = (-1, 1)$ at the maximum. Substituting these values into Eq. (3) yields Eq. (5).

C. Calculation of $\mathbb{P}(D_2^* < R)$

There are 48 ways of assigning values ± 1 and $\pm R$ to two of the entries f_u, f_v, g_u, g_v of J. Integrating the conditions for Turing instability of the remaining entries in each of these cases using Mathematica (Wolfram, Inc.) gives the area of parameter space in which a Turing instability arises,

$$\iiiint_{I^4} \mathbb{1}\begin{pmatrix} J > 0,\ I_1 < 0 \\ p > 0 \\ \max|\mathsf{J}| = R \\ \min|\mathsf{J}| = 1 \end{pmatrix} \mathrm{d}\mathsf{J} = 12(R-1)^2, \tag{S6}$$

where we use the shorthand $\mathrm{d}\mathsf{J} = \mathrm{d}f_u\,\mathrm{d}f_v\,\mathrm{d}g_u\,\mathrm{d}g_v$. To analyze the condition $D_2^* < R$, we note that the expression for D_2^* in Eq. (3) shows that we may swap f_u, g_v and f_v, g_u. Hence the 48 cases reduce to 4 cases (corresponding to the entries ± 1 or $\pm R$ being on the the same or on different diagonals):

(1) $|f_u| = R, |g_v| = 1$; (2) $|f_v| = R, |g_u| = 1$;
(3) $|f_u| = R, |f_v| = 1$; (4) $|f_u| = 1, |f_v| = R$.

Moreover, since $q > 0$, we may take $f_v > 0$ and $g_u < 0$ without loss of generality. We now discuss these cases separately.

(1) $I_1 < 0$ implies $f_u = -R$, $g_v = 1$, and so

$$D_2^* = \left(\sqrt{q} + \sqrt{q - R}\right)^2 \geqslant R. \tag{S7}$$

(2) $f_u g_v = -R$ since $q > 0$, so $J = f_u g_v + R$.

(3) $f_u = -R$ because $I_1 < 0$. Now $p, q > 0$, and so $0 < J = -R|g_v| - |g_u| < 0$. This is a contradiction.

(4) $f_u = 1$ as $I_1 < 0$. Since $g_v \leqslant -1$, it follows that

$$D_2^* = \left(\sqrt{-g_u R} + \sqrt{-g_u R - g_v}\right)^2 \geqslant R. \tag{S8}$$

In this way, $D_2^* < R$ quantifies the diffusive threshold in a natural way. In particular, $D_2^* < R$ is only possible in case (2). Since $J > 0$, we require $f_u g_v + R > 0$ in that case. Now $I_1 < 0$ and $p > 0$, so $1 < f_u < -R/g_v$ or $1 < g_v < -R/f_u$ depending on $f_u > 0, g_v < 0$ or $f_u < 0, g_v > 0$. Assume without loss of generality that $|f_u| \geqslant |g_v|$. Then $f_u < 0$, $g_v > 0$ as $I_1 < 0$. Moreover, using Eq. (3), $D_2^* = R$ if and only if $g_v = 2 + f_u/R$. From Eqs. (S5), D_2^* decreases as g_v increases. Hence

$$D_2^* < R \iff 2 + f_u/R < g_v < -R/f_u \text{ and } f_u + g_v < 0, \tag{S9}$$

bioRxiv preprint doi: https://doi.org/10.1101/2020.11.09.374934; this version posted November 9, 2020. The copyright holder for this preprint (which was not certified by peer review) is the author/funder, who has granted bioRxiv a license to display the preprint in perpetuity. It is made available under aCC-BY 4.0 International license.

using the conditions derived previously. Note that $-R/f_u < R$ and $2 + f_u/R > 1$ for $-R < f_u < -1$. If $|f_u| < |g_v|$, f_u, g_v are swapped in these conditions. Moreover, since $q > 0$, case (2) corresponds to 4 of the 48 cases. Hence we obtain, again using MATHEMATICA,

$$\iiiint_{I^4} \mathbb{1}\begin{pmatrix} J > 0,\ I_1 < 0 \\ p > 0,\ D_2^* < R \\ \max|\mathsf{J}| = R \\ \min|\mathsf{J}| = 1 \end{pmatrix} \mathrm{d}\mathsf{J} = 4\left(\frac{2R(1-R)}{1+R} + R\log R\right). \tag{S10}$$

Eqs. (S6) and (S10) imply

$$\mathbb{P}\left(D_2^* \leqslant R\right) = \frac{R\left[2(1-R) + (1+R)\log R\right]}{3(1-R)^2(1+R)}. \tag{S11}$$

In particular, $\mathbb{P}\left(D_2^* \leqslant R\right) = O(\log R/R) \ll 1$ for $R \gg 1$.

D. Nondimensionalization

We close by remarking on the (absence of) nondimensionalization of the reaction system. Indeed, up to rescaling time, one among f_u, f_v, g_u, g_v can be set equal to ± 1. Moreover, one more parameter can be set equal to ± 1 by rescaling u, v differently. However, if we made those choices, we could no longer sample from a fixed interval.

II. NUMERICAL DETAILS

A. Numerical implementation

Implementing the semi-analytical approach for $N \geqslant 3$ derived in the Letter numerically takes some care as the coefficients of the polynomials that arise can range over many orders of magnitude. Our `python3` implementation therefore uses the `mpmath` library for variable precision arithmetic [S2].

To determine the positive real roots of the polynomials that arise in the semi-analytical approach, we complement the Durand–Kerner complex root finding implemented in the `mpmath` library [S2] with a test based on Sturm's theorem [S3], to ensure that all positive real roots are found. Those systems in which root finding fails—either because the Durand–Kerner algorithm fails to converge or because it finds an incorrect number of positive real roots—are discarded, but included in error estimates where reported.

B. Numerical samples

Table S1 gives the number of random Turing unstable systems from which distributions, averages, and probabilities were estimated for each $R \in \{2.5, 5, 7.5, 10, 12.5, 15, 17.5, 20\}$.

TABLE S1. Number of random Turing unstable systems used to estimate distributions, averages, and probabilities in the main text for the different values of N.

N	binary / non-binary	#(Turing unstable systems)
$N = 2$	non-binary	10^7
$N = 3$	non-binary	10^4
$N = 3$	binary	10^5
$N = 4$	binary	10^5
$N = 5$	binary	$2 \cdot 10^4$
$N = 6$	binary	$2 \cdot 10^3$

SUPPLEMENTAL CODE

The online Supplemental Material also includes parts of the `python3` code that implements the semi-analytical approach for $N \geqslant 3$.

[S1] J. D. Murray, in *Mathematical Biology* (Springer, Berlin, Germany, 2002) Vol. II, Chap. 2, pp. 71–140, 3rd ed.

[S2] F. Johansson, *`mpmath`: a `python` library for arbitrary-precision floating-point arithmetic* (version 1.1.0, 2018).

[S3] C.-K. Yap, in *Fundamental Problems in Algorithmic Algebra* (Oxford University Press, Oxford, England, 2000) Chap. 6 & 7, pp. 141–218.